Journal of South American Earth Sciences 103 (2020) 102708

Contents lists available at ScienceDirect

Journal of South American Earth Sciences

journal homepage: www.elsevier.com/locate/jsames

Basement structural control in the Magallanes-Malvinas Fold and Thrust Belt, offshore Argentina

J.P. Ormazabal [a,b,*], J.I. Isola [a,b], F.I. Palma [a,b], J.G. Lozano [a,b], F.D. Esteban [a,b], M. M. Menichetti [c], E. Lodolo [d], A.A. Tassone [a,b]

[a] Universidad de Buenos Aires, Facultad de Ciencias Exactas y Naturales, Depto. de Ciencias Geológicas, Buenos Aires, Argentina
[b] CONICET - Universidad de Buenos Aires, Instituto de Geociencias Básicas, Aplicadas y Ambientales de Buenos Aires (IGeBA), Buenos Aires, Argentina
[c] Dipartimento di Scienze Della Terra, Vita e Dell'Ambiente, Università di Urbino, Campus Scientifico E. Mattei, 61020, Urbino, FU, Italy
[d] Istituto Nazionale di Oceanografia e di Geofisica Sperimentale (OGS), Borgo Grotta Gigante 42/c, 34010, Sgonico, Trieste, Italy

ARTICLE INFO

Keywords:
Basement step
Stress riser
Magallanes basin
Malvinas Basin
Offshore
Seismic data
Well data
Fold and thrust belt
Basement-involved fault

ABSTRACT

In this study, we examine the external part of the Magallanes-Malvinas Fold and Thrust Belt in offshore areas, including a portion in Tierra del Fuego onshore, in southern South America. Our investigations focus on the interaction between a thin-skinned fold and thrust belt and the basement in that deformation, considering pre-existing structures acting as stress risers and localizing a possible tectonic inversion. The data is composed of around 14,000 km of 2-D multichannel seismic lines and three exploratory wells, used to analyse the anticlines of the fold and thrust belt in the area. The strike of these folds progressively evolves from NW-SE trending in western onshore regions, to WSW-ENE trending in eastern offshore areas. The fold and thrust belt shows a buttressing effect against the Río Chico Arch. The most shortening is seen in the apex of the Río Chico Arch around 67° W, in the coast of Tierra del Fuego, and gradually decreases eastwards in offshore regions. A connection between basement-involved faults and folds offshore is inferred from the analysis of the Géminis and Ciclón anticlines, developed during the N–S last compressional stage of deformation in the late Oligocene/early Miocene. The Géminis anticline is a fault propagation fold with a total shortening of 205 m with a piggyback basin developed over its backlimb. The location and ENE-WSW strike-direction of the fold have been controlled by a basement-involved fault. The Ciclón anticline is a subtle fold trending WNW-ESE developed as a result of the slight tectonic inversion of a negative flower structure.

1. Introduction

The Fuegian Andes are an orogenic belt in morphostructural alignment with the North Scotia Ridge, located around the South American-Scotia plate boundary (Fig. 1). The Magallanes-Malvinas Fold and Thrust Belt (MMFTB) is a complex structure located north of the Fuegian Andes onshore, and north of the North Scotia Ridge offshore. The MMFTB marks the southern limit for the Magallanes (or Austral) Basin onshore and Malvinas Basin offshore, and is described as a thin-skinned fold and thrust belt (FTB, Menichetti et al., 2008; Torres Carbonell et al., 2013). Between the Magallanes and Malvinas basins lies the Río Chico Arch, a Mesozoic aged basement high, which promoted a buttressing effect onshore (Fig. 1; Torres Carbonell et al., 2013; Maestro et al., 2019). Varying strike-directions and development in faults, half grabens and associated basement structures have been observed at each side of the Río Chico Arch (Biddle et al., 1986; Galeazzi, 1998). The conditioning exerted by the basement in the formation of the external FTB has been extensively studied in the onshore region (Torres Carbonell et al., 2017; Maestro et al., 2019). Previous studies have addressed the varying degree of conditioning exerted by the basement features in MMFTB throughout the onshore of Tierra del Fuego. These features include basement steps acting as stress risers and concentrating the location of thrusts and folds of the thin-skinned FTB, and a subtle inversion to the west (Torres Carbonell et al., 2017). In the offshore areas, the knowledge of the structural geometry is relatively scarce and is comprised in basin-scale investigations, or studies referred to other aspects (Robbiano et al., 1996; Galeazzi, 1998; Tassone et al., 2008; Ghiglione et al., 2010; Esteban, 2014; Esteban et al., 2018; Ormazabal et al., 2019). The buttressing effect associated with the Río Chico Arch and the conditioning exerted by the basement in the formation of the MMFTB have not been

* Corresponding author. Universidad de Buenos Aires, Facultad de Ciencias Exactas y Naturales, Depto. de Ciencias Geológicas, Buenos Aires, Argentina.
E-mail addresses: jormazabal@gl.fcen.uba.ar, ormazabaljuanpablo@gmail.com (J.P. Ormazabal).

https://doi.org/10.1016/j.jsames.2020.102708
Received 24 January 2020; Received in revised form 11 June 2020; Accepted 15 June 2020
Available online 23 June 2020

studied in detail offshore.

This study examines the southernmost Magallanes and western Malvinas basins and associated external FTB. Specifically, the last stage of evolution of the MMFTB offshore and the anticlines generated during this phase are the main focus of this study. This includes the analysis of the conditioning exerted in the folds by structures formed in previous tectonic phases. The effect of buttressing exerted by the Río Chico Arch in offshore and its extent are analysed as well. Furthermore, a comparison is made to constrain differences in onshore and offshore regions in the formation of MMFTB and the role played by older basement structures. Finally, this analysis is tied to previous onshore and offshore studies, aiming to relate the configuration of the offshore MMFTB with the evolution of the entire area.

2. Geological background

2.1. Tectonic setting

The current configuration in the southern part of Magallanes and Malvinas basins is a result of the interplay between the South American, Scotia and Antarctic plates (Fig. 1). The main morphostructures in the area are the Fuegian Andes and the North Scotia Ridge. The Fuegian Andes are the southernmost part of the Andean Cordillera, which changes from NW-SE to E-W direction in Tierra del Fuego. In offshore, the Fuegian Andes merge with the North Scotia Ridge. Both structures are located in the transcurrent South American-Scotia plate boundary (SASPB, Fig. 1). The external part of the Fuegian Andes and the North Scotia Ridge is a thin-skinned FTB informally named as Magallanes-Malvinas Fold and Thrust Belt (MMFTB). This fold and thrust belt marks the limit to the west and south of the Magallanes Basin in onshore, and southern limit of Malvinas Basin in offshore, involving the units of these basins in the deformation (Galeazzi, 1998; Menichetti et al., 2008). In onshore, the strike-direction of the MMFTB changes from NW-SE to E-W onshore, and WSW-ENE offshore.

The main tectonic and sedimentary structures of the area are a result of the succession of different tectonic phases, which initiated with the extensional processes in the Triassic/Jurassic (Fig. 2, Biddle et al., 1986). This extension generated the faulting of the late Paleozoic basement, and the consequent generation of grabens and half grabens in Magallanes and Malvinas basins (Baristeas et al., 2013). This fault population has a NW strike in Magallanes Basin (Ghiglione et al., 2013), while further south, the Malvinas Basin has a mainly ENE-WSW to NE-SW trending faults (Baristeas et al., 2013). Between both basins, there is a zone which underwent markedly less faulting and extension, named as Río Chico (or Dungeness) Arch (Biddle et al., 1986; Galeazzi, 1998). The Río Chico Arch is a basement high lying between the two basins that represents the southern prolongation of the Deseado Massif, with a roughly N–S strike; it is a relatively unfaulted region, elevated since its formation in the Mesozoic (Galeazzi, 1998). The offshore region located between MMFTB and the Río Chico Arch is the transitional boundary between the depocenters of both basins (Ormazabal et al., 2019). After the mechanical rifting, a thermal subsidence process was developed during the Cretaceous, with minimal faulting (Ghiglione et al., 2010). In the Late Cretaceous, a change in the regional

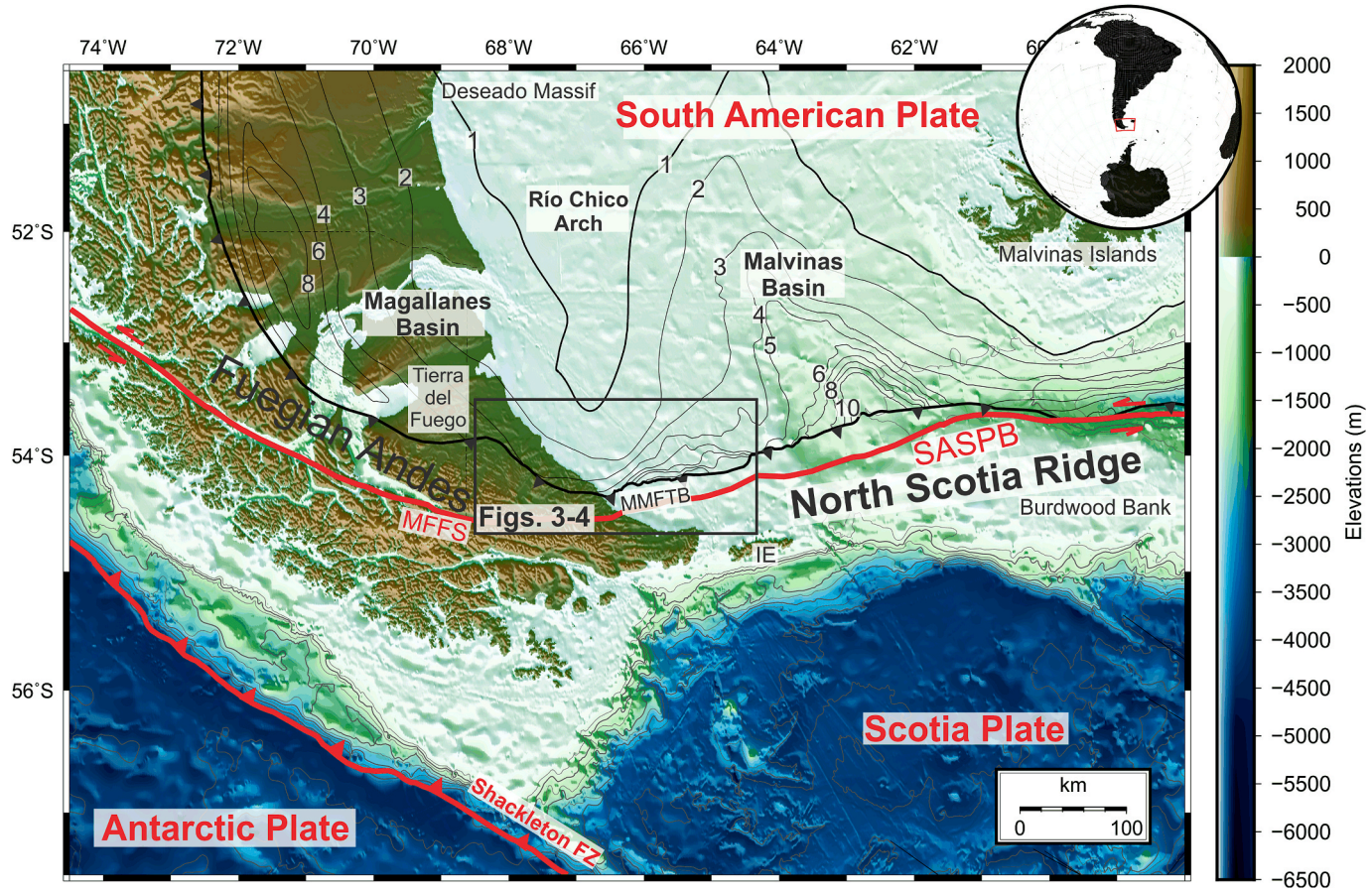

Fig. 1. Bathymetric map of the southernmost South American Plate and northwestern Scotia Plate, showing the location of the Magallanes-Malvinas Fold and Thrust Belt (MMFTB). Sedimentary Thickness for Magallanes and Malvinas basins, contour lines each km, deformational front (black thick line), South American-Scotia Plate Boundary (SASPB; red line), and MFFS (Magallanes-Fagnano Fault System) taken from Ormazabal et al. (2019) and references therein. IE: Isla de los Estados. Red lines depict plate boundaries. Thick black line indicates the localization of the deformation front. (For interpretation of the references to colour in this figure legend, the reader is referred to the Web version of this article.)

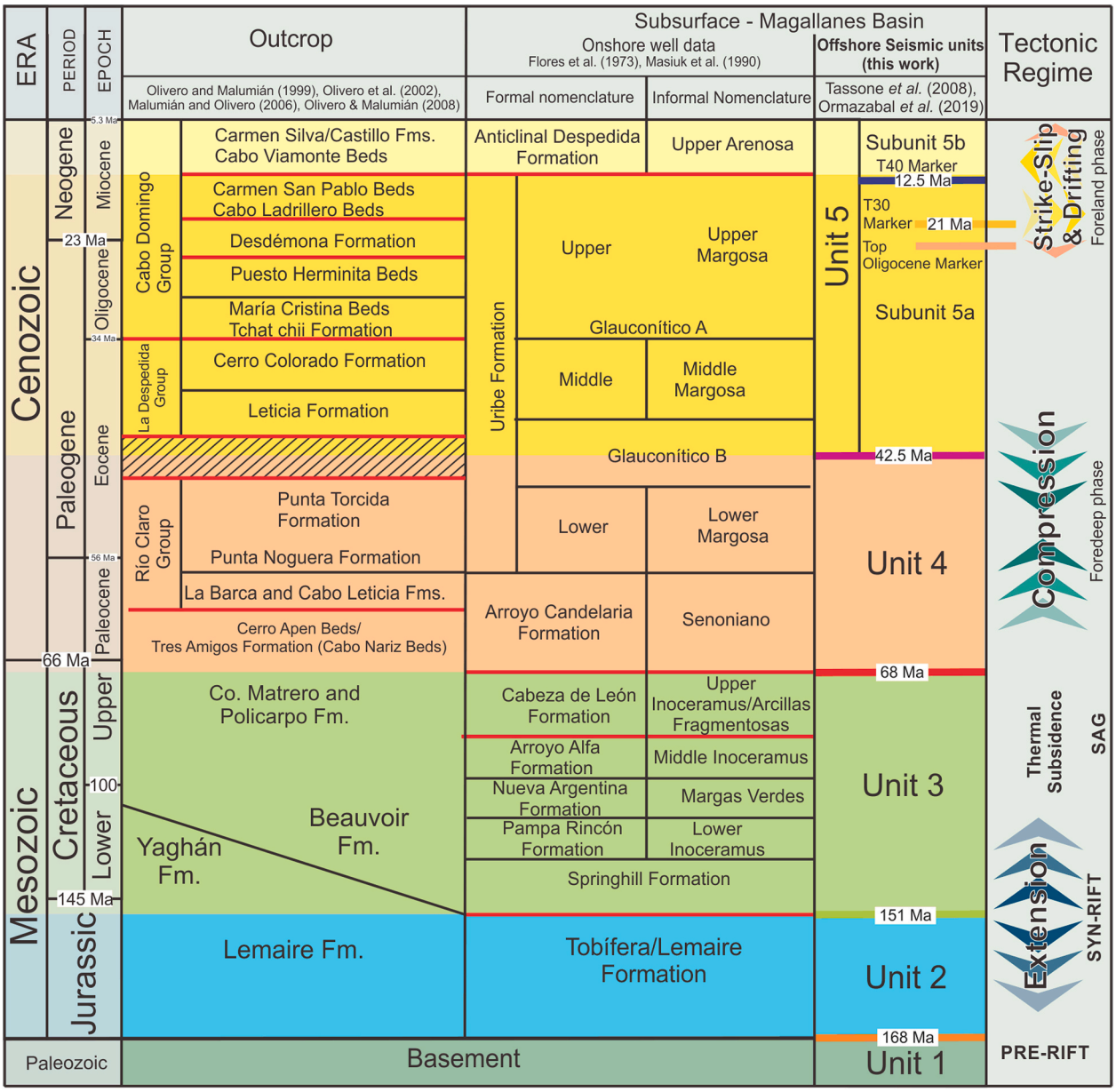

Fig. 2. Stratigraphic Chart with dated unconformities used in this work. Data taken from Olivero and Malumián (1999, 2008), Olivero et al. (2002), Malumián and Olivero (2006), Flores et al. (1973), Masiuk et al. (1990), Tassone et al. (2008), Ormazabal et al. (2019).

geodynamics with convergence between the South American and the Antarctic Plates produced the tectonic inversion of basement rocks (Menichetti et al., 2008), and initiated the first phase of formation of the Andean Cordillera. The compressional tectonic regime prevailed in the region since the Late Cretaceous until the Early Miocene, with several stages (Alvarez-Marrón et al., 1993; Kraemer, 2003; Ghiglione and Ramos, 2005). In onshore regions, Torres Carbonell and Olivero (2019) distinguish two main phases of compressional tectonics since the Cretaceous to the Early Miocene: a first thick-skinned deformational phase during Late Cretaceous-Paleogene (Klepeis and Austin, 1997), and a second thin-skinned deformational phase between latest Eocene to Early Miocene (Torres Carbonell and Dimieri, 2013). For the offshore sector, Galeazzi (1998) made a correlation with the tectonic cycles in onshore, assigning the first compressional phase registered in Magallanes Basin as a "transitional foredeep phase" in Western Malvinas Basin between 68 and 42.5 Ma from regional unconformities. Tassone et al. (2008) support this transtensional transitional phase interpreting a series of negative flower structures in the foredeep of Malvinas basin. Similarly, several authors have widely suggested an extensional/transtensional process at some stage during the Paleogene (Yrigoyen, 1989; Galeazzi, 1998; Tassone et al., 2008; Menichetti et al., 2008; Ghiglione et al., 2010; Baristeas et al., 2013; Sachse et al., 2016; Ormazabal et al., 2019). The emergence of an extensional period in onshore of Tierra del Fuego in Paleogene times was suggested by Ghiglione et al. (2008), although this hypothesis has been rejected by other authors (Torres Carbonell et al., 2013, 2014). For the second phase of structuration, there is a major accordance in a compressional/transpressional tectonic regime for southern Magallanes and Malvinas Basins and the associated FTB as a whole (Ormazabal et al., 2019 and references therein).

The convergence direction during the latest compressional stage has been considered as N–S to NE-SW (Diraison et al., 2000; Torres Carbonell et al., 2013). However, the buttressing effect exerted by the Río Chico Arch in Tierra del Fuego generated a convergence of structures around this feature. This convergence generated a change in the orientation of structures belonging to the MMFTB in Tierra del Fuego from NW-SE to the west inland, to E-W and WSW-ENE to the east along the

coast (Maestro et al., 2019). The buttressing effect is closely associated with the strike-direction and development of folds conditioned by basement steps and associated faults in Tierra del Fuego (Torres Carbonell et al., 2013). Foredeep basement-involved faults have been classified by Torres Carbonell et al. (2017) as Mesozoic extensional faults defining half grabens, which were reactivated due to tectonic loading taking place during the Paleogene compressional phases. The development of the FTB has been divided in different domains, considering detachment levels and thick or thin-skinned deformational styles (Menichetti et al., 2008; Torres Carbonell et al., 2013, 2017) and units involved in deformation (Ghiglione and Ramos, 2005). The anticlines located in the most external part of the FTB (Cagnolatti et al., 1987) have been related to the location of basement steps onshore (Diraison et al., 1997; Torres Carbonell et al., 2011) and offshore (Galeazzi, 1998; Robbiano et al., 1996). The Magallanes FTB has two main decollement levels in onshore Tierra del Fuego developed in Paleocene and lower Cretaceous units, respectively (Ghiglione et al., 2010; Torres Carbonell et al., 2017). Since the early Miocene, the region is dominated by a counterclockwise strike-slip tectonic regime (Ghiglione, 2002; Lodolo et al., 2002).

2.2. Stratigraphy

The units defined in the study area, can be divided using different criteria and classifications (Fig. 2). Given that most of our data are seismic records, this work has taken the division of seismic units made by Tassone et al. (2008) for the offshore of Magallanes and Malvinas basins. Fig. 2 displays a correlation of the offshore scheme with other stratigraphic proposals. Unit 1, the basement of the basins, is composed of upper Paleozoic metamorphic rocks, intruded by Jurassic granites (Yrigoyen, 1989). The variation in the depth of basement top defines the depocenter of the basins (Fig. 1). Unit 2, grouped in the Tobífera Serie, is composed of volcaniclastic deposits (Galeazzi, 1998). The unit rests unconformably over the basement, with the greater thicknesses located within the half grabens; its areal distribution is strongly controlled by the Río Chico Arch (Galeazzi, 1998). Unit 3 was deposited during the sag phase and includes the levels of Springhill Formation related to the flooding of the basin. Its base has been dated in 151 Ma in Patagonia (Biddle et al., 1986), and its top in 68 Ma (Galeazzi, 1998). Unit 4, which unconformably rests over Unit 3 is the thinnest unit and represents the infill during the first phases of compression in Magallanes Basin, and possible transtension towards Malvinas Basin (Baristeas et al., 2013). The unit is wedge-shaped, with its thickest depocenter located to the south. Its top is marked by an erosive surface dated in 42.5 Ma (Galeazzi, 1998), which truncates the upper strata. Unit 5 groups the uppermost levels of the basin. It represents the main unit of foreland basin infill (Biddle et al., 1986). The unit has a well-developed wedge shape (Tassone et al., 2008) and contains three main internal unconformities. The older unconformity, T30, was recognized in the wells Géminis x-1 and Malvinas x-1 and dated at 21 Ma (Fig. 2, Géminis x-1, 2004; Ormazabal et al., 2019). This unconformity is located near the floor of the piggyback basins of the wedge-top zone in offshore Magallanes and Malvinas basins (Ormazabal et al., 2019). The 12.5 Ma unconformity represents the boundary of subunits 5a and 5 b. The youngest unconformity has been dated in 5.5 Ma, and it is particularly well developed in Malvinas basin (Galeazzi, 1998). However, this unconformity is not depicted in this study due to the erosion and/or non-deposition of levels of that age in this zone.

3. Methodology and database

We analysed 14,300 km of 2-D multi-channel seismic reflection profiles, covering an area of 18,000 km^2. The major coverage area corresponds to the offshore section more proximal to the coast (Fig. 3). The recording of the seismic profiles ranges from 3 s to 8 s two-way travel time (TWT). The seismic database has been acquired by oil companies between 1970 and 1998, and provided by the Secretaría of Energía Argentina. Information on the acquisition parameters was not provided for the database. Information regarding the processing parameters for the seismic profiles exhibited in this work is presented in Table 1. The TESAC seismic survey in the offshore of Magallanes Basin, acquired in 1999 for academic purposes was also included (see details in Tassone et al., 2008). Information on the wells Géminis x-1, Ciclón x-1 and Orca x-1 were also provided by the Secretaría de Energía Argentina. The information obtained from the wells was correlated with the main unconformities of the basin, and the top Oligocene and T30 markers (21 Ma).

The interpretation of the seismic profiles was made with the IHS Kingdom Software (v. 2015). This interpretation included picking horizons equivalent to the main seismic units. The horizons top of Unit 1 (Basement) and Top Oligocene marker were gridded to obtain a grid in time domain.

Several seismic profiles have been scaled from time to depth with the software Depth Converter (v. 2.4; http://users.chariot.net.au/~witek/t2d.htm). The velocity model used has been taken from check shot information of the wells Ciclón, Orca and Géminis (Table 2). This velocity

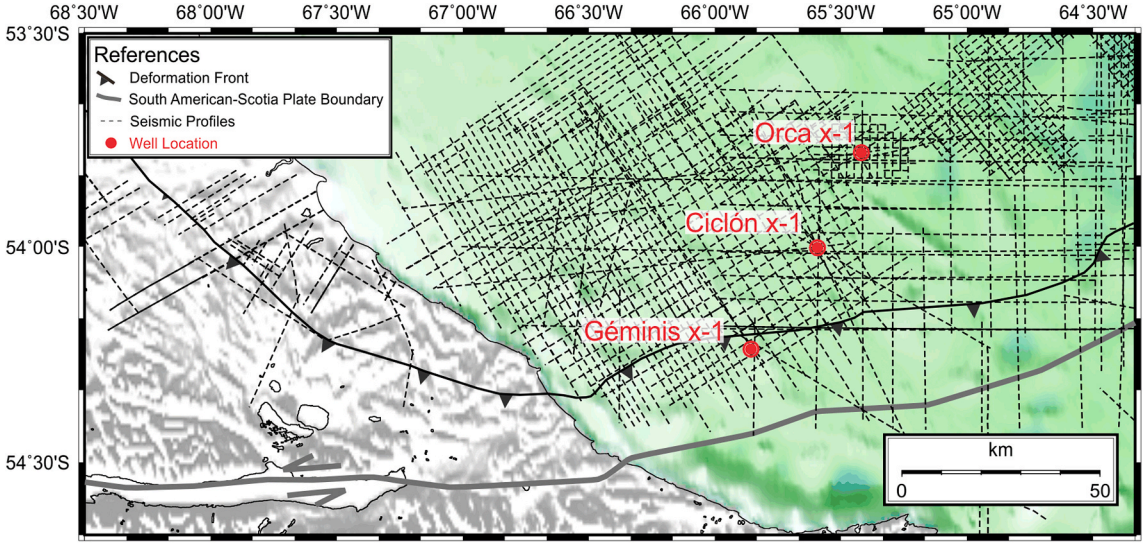

Fig. 3. Database for this study, composed of seismic lines and well data. See location in Fig. 1.

Table 1
Seismic data processing flow.

PROCESSING FLOW
Reading and conversion of data to internal format
Geometry allocation and quality control
Attenuation of random noise and ocean waves noise and resampling at 4 msec
Correction for register delay, source depth and receivers
Spherical divergence correction
Attenuation of water-bottom multiples
Deconvolution and amplitude balancing
First velocity analysis
Radon transform 2nd pass
Second velocity analysis
Migration velocity model-building
Analysis of the normal move out residuals on the migrated gathers
Kirchhoff pre-stack time migration (PSTM)
Front mute, filters and gains
Seismic signal sum
Image enhancement methods

model was applied individually for each seismic profile and used to obtain the top basement and top Oligocene depth maps. For some seismic profiles, a Pseudo-Relief Attribute (TecVA, Bulhões and de Amorim, 2005) was calculated, with the aim of highlighting the acoustic arrangement and structures (especially faults) subtly observed in a regular seismic profile. The application of the Pseudo-Relief Attribute helped with the interpretation of reflectors and faults. A balanced restoration was made for the seismic section depicted in Fig. 7 using the software Move 2017. The grids and figures presented in this work have been made with Generic Mapping Tools software (GMT v.5; Wessel et al., 2013) and CorelDraw X7.

4. Structure

The MMFTB in Tierra del Fuego both onshore and offshore is composed of a series of folds and thrusts affecting units formerly belonging to Magallanes and Malvinas basins (Figs. 4–6). Basement-involved faults are widespread throughout the basins (Fig. 4). The development of the faults started in the Mesozoic, as can be observed in the change of thickness of the Units 2 and 3 on either side of these faults (Figs. 5 and 7). Fault displacements increase southwards, in the foredeep, defining large basement steps. These basement steps set up abrupt changes in the depth of the basement top (Fig. 4). A few basement-involved faults could be recognized below the most external part of the FTB (Fig. 7). Some anticlines in the FTB overlay and mimic the location of these basement-involved faults (Fig. 4).

From a regional point of view, the deformational front, external FTB folds and basement-involved faults follow the contour of the Río Chico Arch, roughly depicted in the top basement map (Fig. 4). The strike of the deformational front onshore is NW-SE, whereas in the offshore region is dominantly ENE-WSW, with the inflection point located around the 67° W, as displayed in the change of fault strike-directions. The strike of folds changes progressively from a NW-SE dominant orientation in western onshore, to a ENE-WSW dominant orientation for the offshore area. In the eastern onshore region, the outcropping structures have an E-W to ENE-WSW direction (Olivero and Malumián, 1999; Torres Carbonell et al., 2013; Maestro et al., 2019). The onshore-offshore change in the strike of basement-involved faults is less pronounced than the change in the strike of folds. In onshore, the basement-involved faults have a main NW-SE to WNW-ESE strike, whilst in offshore it is E-W to ENE-WSW, especially near the FTB. Additionally, towards the offshore foredeep, several basement-involved faults WNW-ESE strike-oriented are observed.

4.1. Offshore sector

The analysed offshore area belongs to the most external MMFTB and southern foreland basin. The FTB is located from the deformational front southwards to the hinterland, and the foreland basin from the deformational front towards the foreland. The main structures in the area are the anticlines Géminis and Ciclón, each one with a basement-involved fault associated. Despite the chaotic acoustic arrangement in the FTB, some other folds were identified in the FTB, together with a piggyback basin developed over the backlimb of the Géminis anticline (Fig. 6).

4.1.1. Géminis Anticline, associated basement-involved fault and piggyback basin

The most external FTB anticline is informally named Géminis anticline, after Géminis x-1 well, drilled near the hinge of the fold (Fig. 7). The Géminis anticline is the most external FTB fold, hence the deformation produced by the development of this anticline defines the deformational front. The anticline has an amplitude of 400 m with a wavelength of 6 km, and at least 50 km in length with an ENE-WSW strike (Figs. 6 and 7). The forelimb is slightly more tilted than the backlimb, indicating a NNW vergence. Due to the asymmetry between the two limbs and the location in the most external region of the FTB, the anticline deformation mechanics have been related to fault-propagation folding.

The anticline involves levels of the Units 4 and 5. The top of pre-deformational strata is located stratigraphically near the Top Oligocene marker. The Géminis anticline is developed above a decollement level located over the boundary between Units 3 and 4. Units 4 and 5 are dominated by claystones, interbedded with some sandstones levels that are fully involved in the folding (Géminis x-1 report, 2004).

The blind thrust that produces the folding propagates upwards, cutting through unit 4, and reaching the lower levels of unit 5. Below the anticline, there is a basement step, associated with a main basement-involved normal fault, dipping to SSE (Figs. 6 and 7). This normal fault has an ENE-WSW strike, coincident with the Géminis anticline strike. There is an inferred connection between the thrusting and the basement-involved fault, in the zone with acoustic noise (Fig. 7). This fault seems to affect the basement, Units 2, 3 and lower levels of Unit 4, which is indicative that the fault was active until at least the middle Eocene.

The hinge of the Géminis anticline is collapsed, and the backlimb is slightly higher than the forelimb. This decoupling between limbs is led by a SSE high tilted thrust, which affects Unit 5 (Fig. 7). The roots of this

Table 2
Velocity model and time to depth conversion for each seismic profile. The spot in which the conversion was applied is indicated below the name of the figures.

Unit	Velocity (m/s)	Horizon	Fig. 5 (Km 25)		Figs. 7–8 (Km 20)		Fig. 8b (Km 11)		Fig. 10 (Km 26.5)		Fig. 12 *Onshore* (Km 10)	
			TWT (ms)	DEPTH (m)	TWT (ms)	DEPTH (m)	TWT (ms)	DEPTH (m)	TWT (ms)	DEPTH (m)	TWT (ms)	DEPTH (m)
Water	1500	Sealevel	0	0	0	0	0	0	0	0	–	–
5	2780	Seabed	104	78	122	92	100	75	132	99	–	–
4	4255	Top U4	2629	3588	2805	3821	2670	3647	3129	4265	1200	1668
3	3240	Top U3	3354	5130	3262	4793	3549	5517	3825	5746	2234	3868
2	2923	Top U2	4065	6282	4017	6016	3941	6152	4604	7008	2590	4445
1	–	Top U1	4378	6739	4426	6614	4248	6601	5038	7642	2790	4737

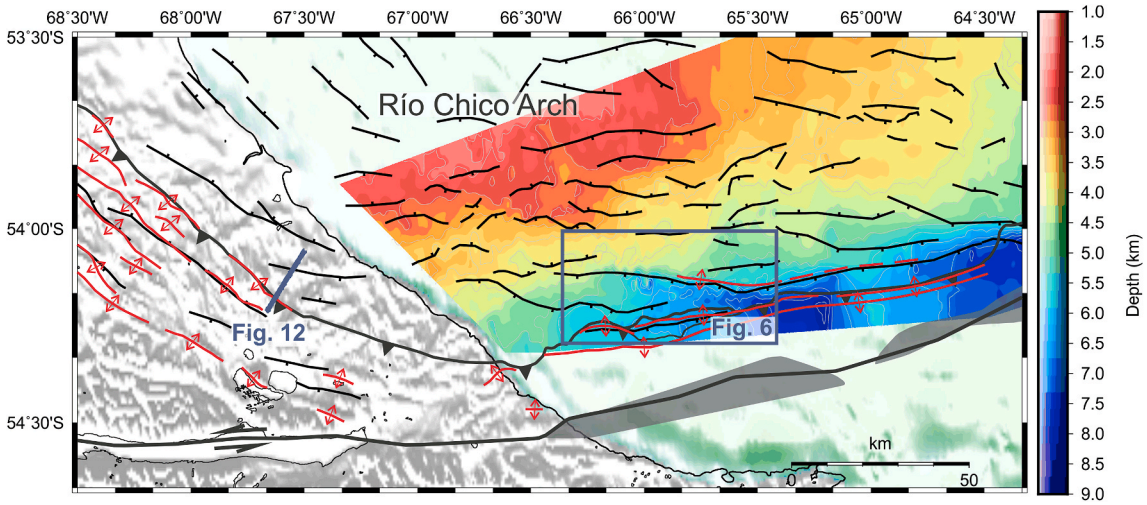

Fig. 4. Onshore-offshore Magallanes-western Malvinas basin structural map. See location in Fig. 1. The offshore section is completed with a basement depth map and associated MMFTB. The entire area depicts the main structures, including anticlines (red lines) and faults affecting the basement. Black solid lines show the FTB deformational front and the South American-Scotia plate boundary, with a series of associated strike-slip basins, depicted as dark grey polygons. Red dashed line represents the locations where Ciclón Anticline cannot be easily recognized. Offshore basement-involved faults have been obtained in this work. Onshore and north offshore faults location taken from Diraison et al. (1997), Menichetti et al. (2008) and Ghiglione et al. (2013). Onshore anticlines location taken from Torres Carbonell et al. (2017). Strike-slip basins contour taken from Esteban et al. (2018). (For interpretation of the references to colour in this figure legend, the reader is referred to the Web version of this article.)

thrust cannot be clearly defined. In addition, the rest of analysed seismic profiles do not depict a greater development of this thrust, and some of them do not show it. The collapsed anticline hinge has a set of crestal faults likely rooted in the thrusting that decouples the limbs of the Géminis anticline, through a major subvertical crestal fault (Figs. 7 and 8). The crestal faults seem to have the same strike as the anticline, and are bivergent, dipping to the NNW and SSE. Furthermore, the arrangement of postdeformational levels shows a double progradation direction to the hinge of the Géminis anticline, from the hinterland and foreland.

The shortening generated by the formation of the Géminis anticline was calculated in a section of 6 km (Fig. 9). The main features considered for the restoration were the frontal thrust, and to a lesser degree the inner thrust, together with the associated unfolding. The restoration was divided in one early Miocene step, and two intra Oligocene steps. The restoration of the step 1 corresponded to the restoration of the slight displacement of the thrust located in the hinge of the Géminis anticline (Fig. 9A). The restoration belonging to the Oligocene corresponded to the steps 2 and 3. The step 2 consisted in the restoration of the displacement along the main thrust that defines the Géminis anticline, together with the unfolding of the Top Oligocene marker (Fig. 9C). The step 3 applied the same mechanism than the step 2 in a level located below the Top Oligocene marker (Fig. 9D). From the levels unfolded in the last step, it can be inferred a late Oligocene age for the first phase of thrust and folding in the Géminis anticline. The shortening obtained for the Géminis anticline is 205 m (3.3%). The restoration did not consider a basement inversion, though it could have happened.

The syndeformational deposits located over the backlimb, between the hinge of the Géminis anticline and an internal thrust (Fig. 8A) represent the sedimentary fill of a piggyback basin. The basin has a length of 25 km, a maximum width of 4 km and a maximum thickness of 500 m. The extension of the piggyback basin can be inferred as the distance between the Géminis anticline and the folds located to the south of the basin (Fig. 6). The syndeformational deposits span from upper Oligocene, to lower Miocene (Fig. 8A), which constrain the last event of compression/transpression in the area. The deposits within the piggyback basin can be divided stratigraphically by the markers recognized from the well Géminis x-1. The sedimentary package A (Fig. 8) overlies the marker top Oligocene, and its top is the T30 marker; the arrange of reflectors is characterized by a subtle onlap over the backlimb of Géminis, with NNW propagation direction. The sedimentary package B is constituted by syndeformational deposits onlapping the marker T30 with direction of propagation NNW as well. The upper levels of package B are truncated by a Miocene aged unconformity. Claystones to silty claystones with sandstones intervals characterize this package in the location of the Géminis x-1 well (Fig. 7).

The southern boundary of the piggyback basin is not clear, due to the scattering of seismic energy related to the small-scale structures resulting from the deformation in the FTB and/or the reflections associated with the ocean bottom reflector. However, the deposits of the piggyback basin in such sector are syndeformational with respect to the formation of an anticline, whose forelimb acts as the southern limit of the piggyback basin (Fig. 8B). The syndeformational levels affected in the southern piggyback sector seem to be slightly younger than syndeformational levels northwards over the Géminis anticline. Due to this age difference, the thrust that generates the southern anticline could be interpreted as an out-of-sequence structure, disturbing the infill of the piggyback basin (Fig. 8B).

To the west, the Géminis anticline is less developed in amplitude, to the point that it cannot be recognized west of 66° W and the piggyback basin is connected with the foredeep deposits without interruption by foldings. Conversely, towards the east the limbs of the Géminis anticline are closer than in the central piggyback basin sector (Fig. 8), together with a smaller distance with the next internal anticline. Syndeformational deposits over the backlimb of the Géminis anticline could not be observed east of 65° 40′ W (Fig. 10).

4.2. *Ciclón anticline and associated flower structure*

The deformation in the foredeep is clearly controlled by structures that involve the basement. The most outstanding feature is a negative flower structure (Menichetti et al., 2008; Tassone et al., 2008; Ormazabal et al., 2019) which acts as a limit for the main foredeep depocenter (Fig. 10 y 11). This structure is continuous eastwards towards Malvinas Basin (Ormazabal et al., 2019 and references therein). The structure has a variable strike: to the west of the 65° 30′ W, the main fault has a WNW-ESE strike, and is controlled by a main SSW tilting fault and, to the east of 65° 30′ W, the structure has ENE-WSW strike, and is controlled by a main SSE tilting fault (Figs. 4 and 6). This main fault bounds the

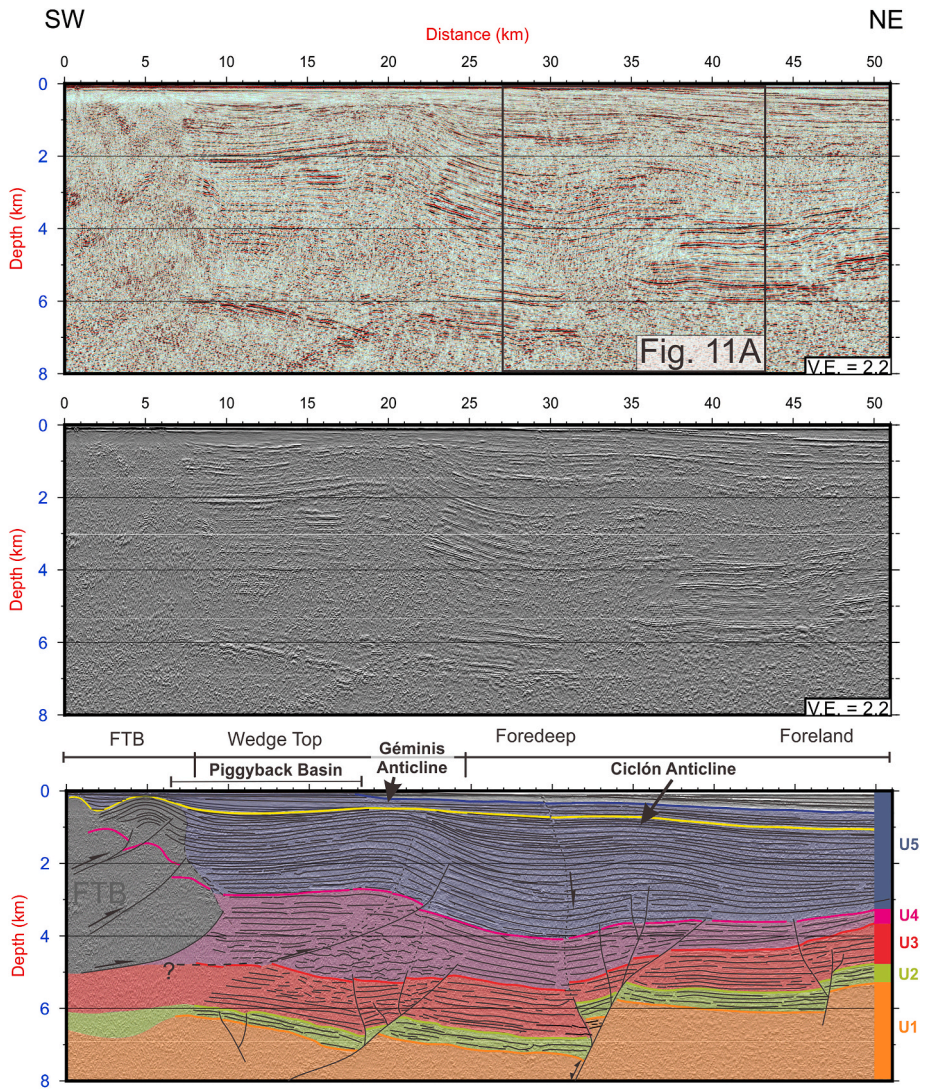

Fig. 5. Multichannel Seismic line (upper) processed with TecVA (middle, Bulhões and de Amorim, 2005) and interpretation (below) depicting the configuration of the external FTB and foredeep. It is evident the association between basement-involved faults with Ciclón and Géminis anticlines. See location in Fig. 6. V.E: Vertical Exaggeration.

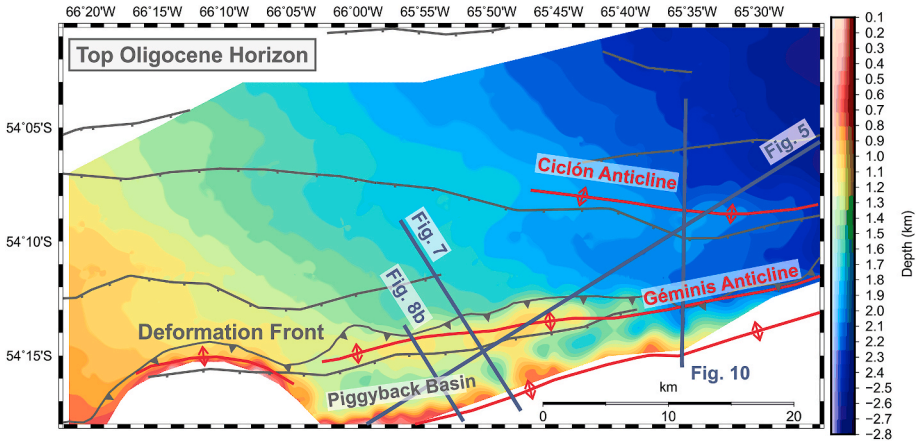

Fig. 6. Top Oligocene depth map, depicting the morphology of upper predeformational strata. Three main folds hinges outstands: The external corresponds to the Ciclón Anticline, located in the Foredeep; The Géminis Anticline is associated with the deformational front; The inner fold, located to the south of the Géminis Anticline, is the most internal fold depicted on the seismic lines. Top Oligocene levels show the floor of the piggyback basin located between the Géminis anticline and the inner fold. See location in Fig. 1.

basement high located to the foreland and produces a displacement which affects Unit 1 (basement) to lower levels of Unit 5. The maximum displacement is around 1 km for Units 1 to 3. An important displacement is observed for the lower levels of Unit 4, together with a significant change in thickness at each side of the fault (with 750 m of slip). The faulting slightly affects the lower part of Unit 5.

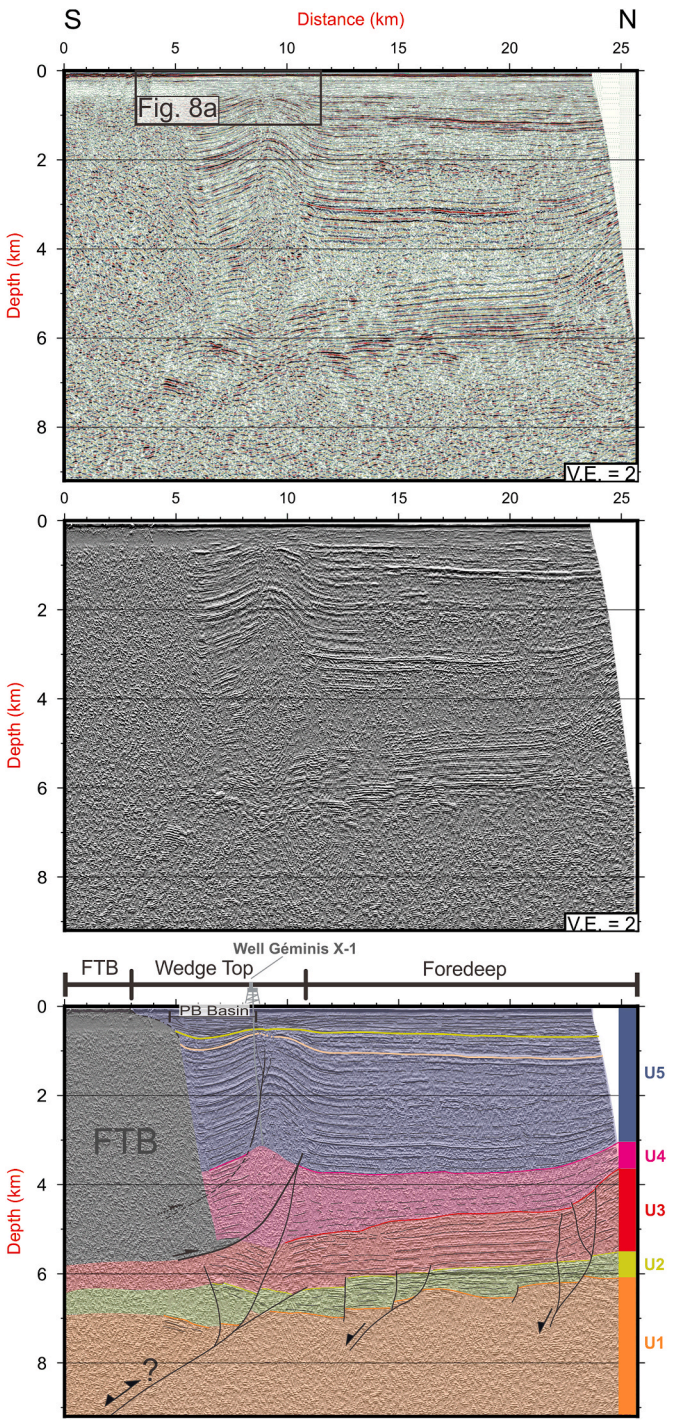

Fig. 7. Multichannel Seismic line (upper) processed with TecVA (middle, Bulhões and de Amorim, 2005) and interpretation (below) depicting the Géminis anticline and associated structure. See location in Fig. 6. V.E: Vertical Exaggeration.

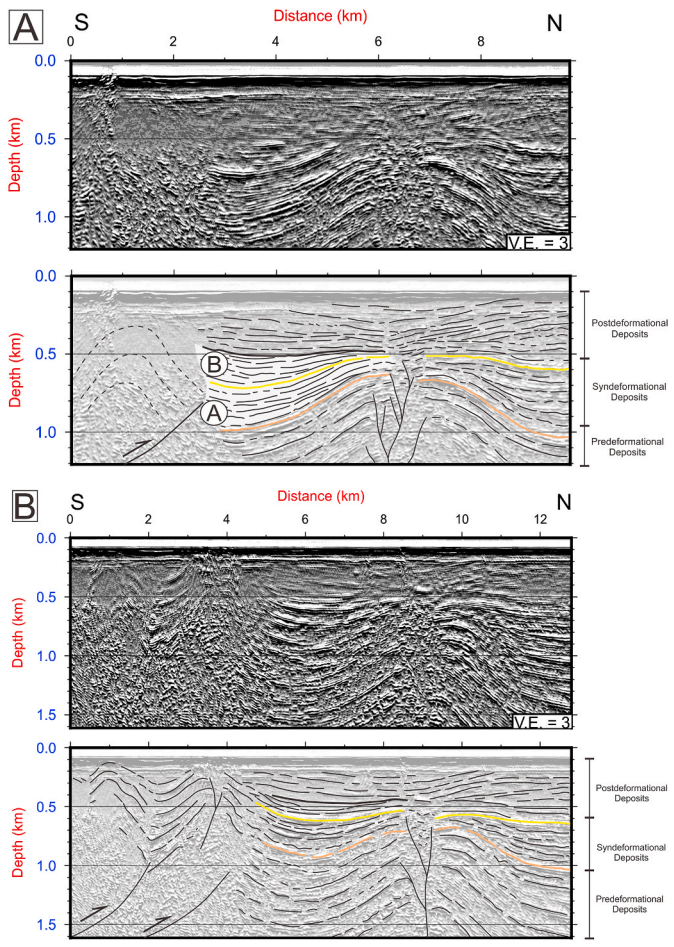

Fig. 8. Multichannel Seismic lines processed with TecVA (upper, Bulhões and de Amorim, 2005) and interpretation (below) depicting the outermost part of the MMFTB around the Géminis Anticline. V.E: Vertical Exaggeration. A) Top Géminis Anticline and associated piggyback basin in grey. See location in Fig. 7. B) Top piggyback basin syndeformational deposit marked with thick black line. See location in Fig. 6.

A very open fold is developed over that flower structure (Fig. 11). The fold, informally named Ciclón anticline (due to the near Ciclón x-1 well), follows the strike of the flower structure for 50 km (Figs. 4 and 6). The Ciclón anticline has a very subtle amplitude, with maximum values of 170 m in the top of predeformational levels (Top Oligocene marker), and a wavelength of 6 km. The folding of reflectors associated with the anticline progressively decreases over the Top Oligocene marker, to the point that the folding cannot be observed in reflectors located over the T30 marker (Fig. 11). The Ciclón anticline is likely the result of a slight inversion of the SSW faults of the flower structure, including the master fault. The amplitude of the anticline is larger around 65° 35′ W and decreases both eastwards and westwards. To the west, the fold cannot be recognized west of 66° W. To the east, the amplitude and mainly the wavelength of the anticline varies markedly, such that it is not be observed in every seismic profile, and its development is very subtle. In seismic profiles east of 64° 40′ W, the development of the flower structure is greater, but the anticline does not exist (Esteban et al., 2018). However, towards the easternmost area of this study (Fig. 4), an inversion associated with the same fault that controls the location of the Ciclón anticline can be observed (Ormazabal et al., 2019).

5. Discussion

MMFTB shows a fairly good continuity between offshore and onshore areas, at each side of the Río Chico Arch. However, some specific differences between the features of each domain are observed, specifically in the southern areas of Magallanes and Malvinas basins. The seismic profiles for both areas show a deformation front delimited by folds, influenced by basement steps, which worked as stress risers (Figs. 7 and 12). In the most external part of the FTB, anticlines as Buenos Aires and Rubí onshore (Fig. 12; Lozano et al., 2020), and Géminis and the most internal anticlines offshore (Figs. 5 and 7) show similar geometries with similar genetic mechanism. In both cases, there are basement-involved faults conditioning anticlines location (called "X

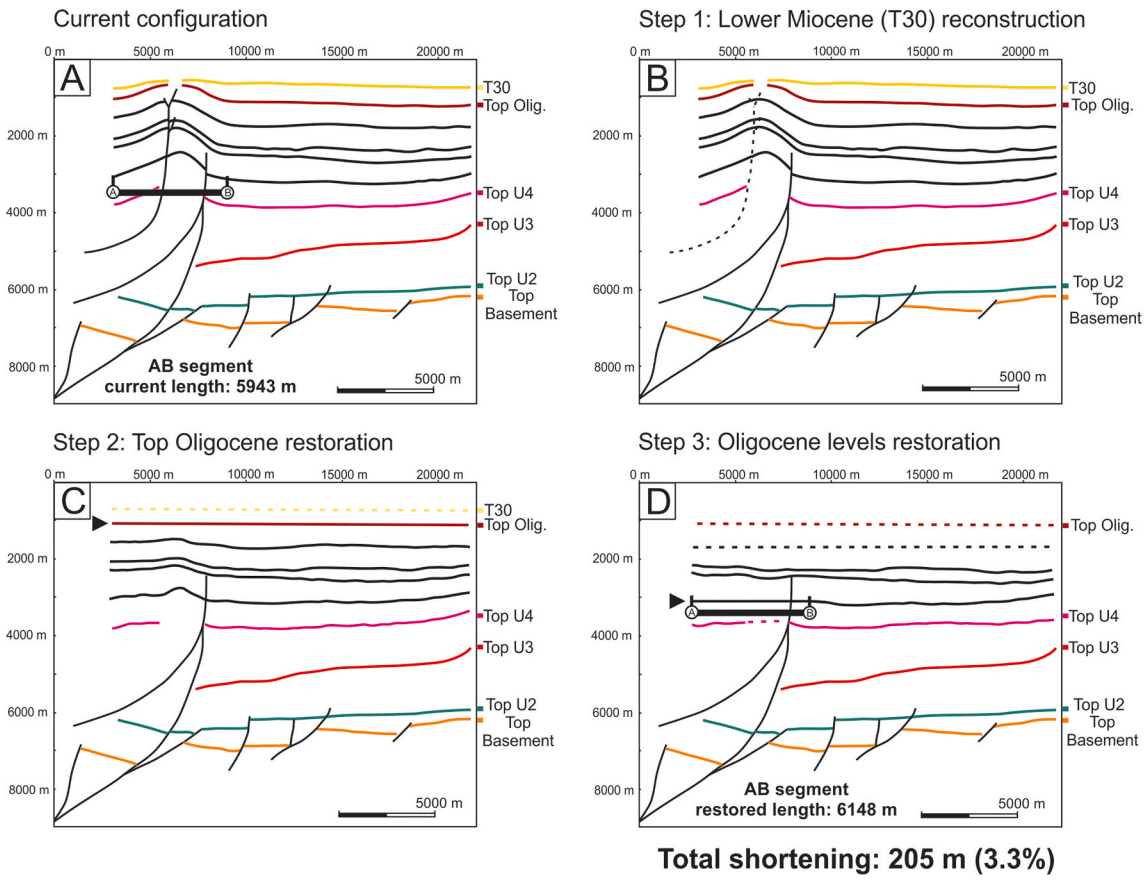

Fig. 9. Balanced section of the Géminis Anticline.

fault" in onshore below the Buenos Aires anticline in Torres Carbonell et al., 2017). Another remarkable feature is the fault located in the foredeep of Magallanes and Malvinas basins in both onshore and offshore regions. The most significant feature observed in the offshore foredeep is the flower structure below the Ciclón anticline. Its counterpart in the onshore is an extensional fault located in the foredeep, named as "Z fault", by Torres Carbonell et al. (2017). The authors suggested a late Eocene age for the last activation of such fault, based in the displacement observed in the lower levels of the unit 4 and the associated growth strata over the top lower Margosa marker (Fig. 12).

5.1. Structural comparison between onshore and offshore in MMFTB

In Tierra del Fuego, Maestro et al. (2019) defined, from fault population analysis, a variation of compressional stress field direction from NE-SW to NW-SE from west to east, respectively. These authors interpreted this difference as due to the indentation generated by the Río Chico Arch. Previously, Torres Carbonell et al. (2011, 2013) studied and specified this interaction as a buttressing effect exerted by the Río Chico Arch. This effect is viewed in the change from a gentle deformation with large-wavelength folds in the western onshore region, to structures with more tight geometry and closer folds in the coast, evidence of greater shortening there.

The absence of seismic profiles in the coast of Tierra del Fuego does not allow the comparison of the relationship between basement and FTB there, but outcrop studies dealt with a structural high of Paleocene age (Torres Carbonell et al., 2008). In eastern Tierra del Fuego inland, the role played by the basement in the deformation has been assigned mainly to basement steps acting as stress risers, and a possible subtle inversion of Mesozoic basement-involved faults. Conversely, in western Tierra del Fuego inland the inversion of basement structures has been observed (Torres Carbonell et al., 2017).

Offshore, the seismic lines covering Géminis and Ciclón anticlines show the syndeformational strata as young as lower Miocene (T30: 21 Ma, Ormazabal et al., 2019), coincident with the ages of similar deposits onshore (Torres Carbonell et al., 2008). The Géminis anticline has been defined in this work as a fault propagation fold, containing the location of the deformation front. The location of the fold, controlled by a basement step, seems to confirm the influence of basement steps acting as stress risers (Fig. 7). The location of the Géminis anticline mimics the location of the basement-involved fault, which is not necessarily the case for the rest of the FTB. Therefore, the control exerted by the basement favored the formation of the piggyback basin.

The shortening obtained for the Géminis anticline is low (3.3%). Nonetheless, this shortening is still comparable with structures located in the outermost part of the Magallanes FTB, especially in Tierra del Fuego inland (Table 3). The magnitude of the Géminis anticline can be assumed to be equivalent to the outermost structures observed towards the west of Tierra del Fuego inland, where the buttressing effect produced by the Río Chico Arch is lower than in the coast. In the coastal zone, the outermost MMFTB shortening is nucleated in the Punta Gruesa imbricated system. There, the shortening is significantly greater than in the Géminis anticline (Table 3).

Several studies have estimated the magnitude of shortening for the Fuegian Andes in Tierra del Fuego. The maximum shortening measured reaches 35 km for the cover in the Chilean sector (west of 68° 30' W), whereas the eastern sector has maximum shortening magnitudes of 59 km for the sedimentary cover (Table 4).

Despite the low shortening calculated for the Géminis anticline, it is necessary to point out that this estimation has been made for a sole structure. The seismic profiles analysed in this work depict other structures associated with folds and thrusts towards the hinterland

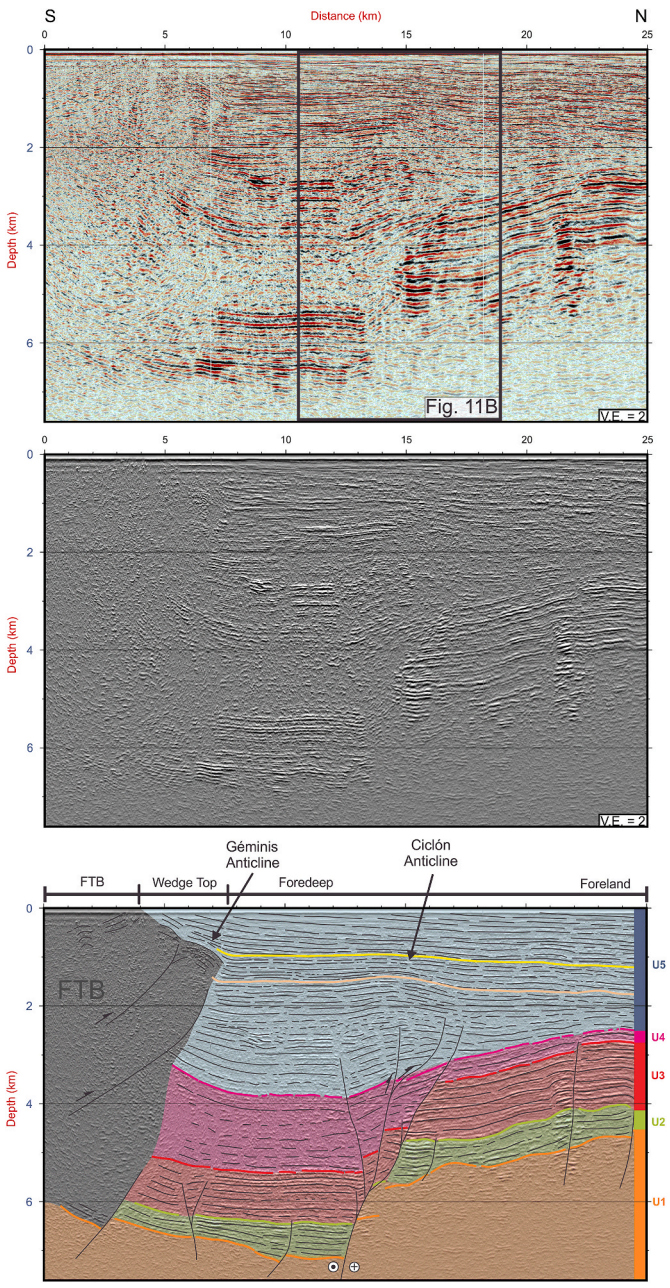

Fig. 10. Multichannel Seismic line (upper) processed with TecVA (middle, Bulhões and de Amorim, 2005) and interpretation (below) depicting the Ciclón anticline and associated basement-involved fault. The levels affected by the negative flower structure (km 14) span from Unit 1 to lower levels of Unit 5. The thickness change in Unit 4 and lower levels of Unit 5 is explained by the activity of the transtensional structure. In the flower structure below Ciclón Anticline, the transpressive fault cinematic is indicated with black arrows. In the km 7, the Geminis anticline is recognized. Below Géminis anticline, it is inferred the presence of its associated basement-involved fault, which is dimmed due to the acoustic noise resulting from the deformation in the FTB. V.E: Vertical Exaggeration.

(Fig. 8b). These internal anticlines could not be included in the shortening estimation due to the limitation of the seismic information there. Thus, the low shortening calculated is just the most external expression of a greater shortening resulting from the deformation of the FTB during the Paleogene. Since the dimensions of the Géminis anticline are clearly different to more internal parts of the FTB, its shortening percentage does not reflect the shortening of the entire MMFTB for that sector. From observations of structures in the hinterland, it can be inferred that the shortening percentage for the entire MMFTB across the Géminis anticline latitude should be greater than the calculated. At the same time, the magnitude of the shortening could be similar to the proximal shortening calculated in the coast by Torres Carbonell et al. (2013). For the analysed section of the Géminis anticline and the associated portion of MMFTB, the most probable value could be extrapolated from the adjacent sector of easternmost Tierra del Fuego, proximal to the coast (Table 4; Torres Carbonell and Dimieri, 2013), yielding a value of around 46 km for the FTB. However, the Géminis anticline has significantly less shortening than frontal structures in Tierra del Fuego coast (Torres Carbonell et al., 2008, 2013). This would indicate that the greater shortening due to the buttressing exerted against the Río Chico Arch is located in the coast and decreases to the east. Additionally, the similarity between the Géminis anticline and the structures of Tierra del Fuego inland, indicate a greater shortening in the Tierra del Fuego coast, which decreases both towards east and west.

A shift in the stress directions was proposed in Tierra del Fuego onshore converging around the Río Chico Arch with a change from NE-SW compression in western areas to NW-SE in eastern ones (Maestro et al., 2019). Considering the strike of folds along the offshore studied area (Fig. 4), the direction of compression should be roughly N trending, generating E-W oriented structures. This direction of compression would generate compressional structures with E-W strike. The strike of the Géminis anticline (ENE-WSW) and the Ciclón anticline (WNW-ESE) deviates from an E-W orientation, due to their orientation inherited from the direction of the associated ancestral basement-involved faults.

5.2. *Structural comparison between onshore and offshore in the foredeep*

The Ciclón anticline was interpreted as the result of the upper Oligocene/lower Miocene transpressional/compressional subtle inversion of an Eocene negative flower structure (Fig. 11). The expression of a Paleogene transtensional/extensional phase in Tierra del Fuego onshore is controversial (Menichetti et al., 2008; Ghiglione et al., 2008; Torres Carbonell et al., 2011). Torres Carbonell et al. (2017) attributed the extensional displacement observed in the onshore foredeep fault "Z" (Fig. 12; see section 5.1) to the tectonic load produced due to the rise of the Andean Cordillera. Although we agree with this interpretation in the onshore region, the foredeep faults suggest a simpler structure and markedly less displacement onshore than the flower structure below the Ciclón anticline in offshore regions. Furthermore, the greater displacement of basement faults in the foredeep offshore is hard to explain as generated only by tectonic load (Ghiglione et al., 2010). This large displacement has been suggested by Galeazzi (1998) to have been caused by a Paleogene transtensional process, which created an E-W trough in the foredeep (Fig. 10). Stratigraphic studies of Magallanes and Malvinas basins agree with an extensional process during the Paleocene-Eocene towards south of Malvinas Basin (Baristeas et al., 2013; Sachse et al., 2016; see section 2.1 for details). From the data analysed in this work, we support that a transtensional process would have taken place eastwards of Río Chico Arch in offshore Magallanes and Malvinas basins.

At the onset of the FTB building during the Oligocene, the structures in the foredeep show the development of the Ciclón Anticline, instead of an extensional displacement due to tectonic load. This slight inversion was suggested in this structure by Menichetti et al. (2008). The Paleogene inversion of Mesozoic aged normal faults has been mentioned by Galeazzi (1998) in the foredeep area as well. The author describes several anticlines generated from the inversion of basement-involved faults and suggests an inversion age spanning from late Eocene to early Miocene. Our work agrees with an early Miocene age for the younger units involved in the formation of the Ciclón anticline.

6. Conclusions

The aim of the present study was to examine the last phase of

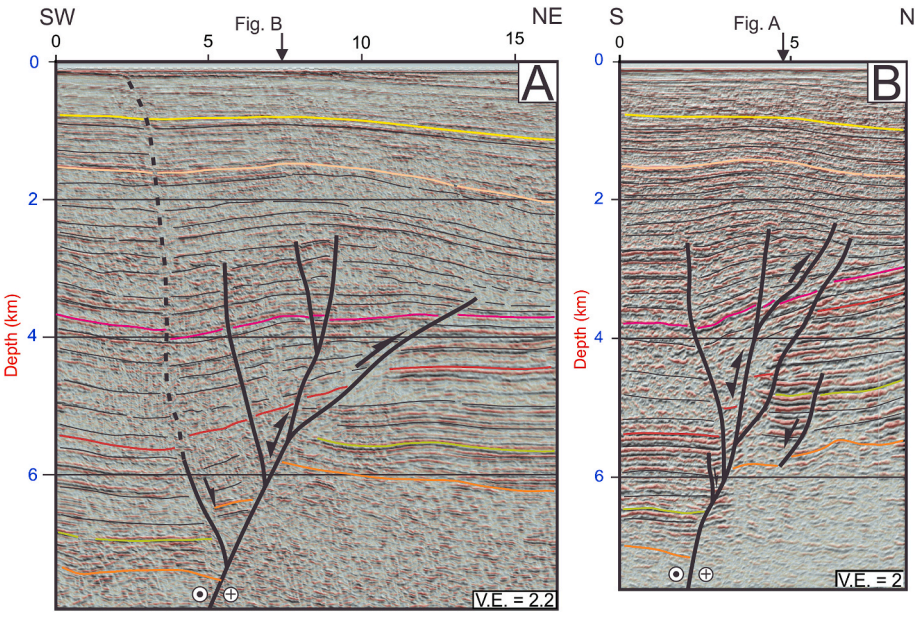

Fig. 11. Details of multichannel seismic lines combining amplitude and Pseudo-Relief Attribute (TecVA attribute, Bulhões and de Amorim, 2005) showing the possible inverted flower structure in the foredeep, viewed in two cross-sections of different orientation. The inset A cuts the structure obliquely, generating an apparent lesser angle of faults than the orthogonal cut by inset B. Dashed line in inset A depicts an inferred extensional fault. See location for inset A in Fig. 5 and inset B in Fig. 10.

Table 3
Shortening magnitudes calculated across MMFTB.

Reference	Location	Structure	Shortening	Original length	Distance of transect to Géminis
Torres Carbonell et al. (2013)	Tierra del Fuego coast; outcrop	Punta Gruesa Imbricated system	1350 m; 22%	6.07 km	40 km along strike
	Tierra del Fuego inland; subsurface	Frontal anticline	152 m; 1.8%	8.3 km	140 km
		Frontal anticline rooted in a backthrust	499 m; 3%	16.499 km	
		Despedida and associated anticline	431 m; 3%	14.26 km	
This work	Offshore Tierra del Fuego	Géminis anticline	205 m; 3.3%	6.15 km	–

Table 4
Previous studies for shortening estimation in Tierra del Fuego.

Reference	Shortening		Minimum distance to Géminis	Age of deformation
	Basement	Cover		
Alvarez-Marrón et al. (1993)	–	30 km (60%)	175 km	Oligocene to older
Kley et al. (1999) modified from Alvarez Marrón et al. (1993)	59 km (41%)	35 km (40%)	175 km	Paleocene or younger
Rojas and Mpodozis (2006)	14–18 km (20%)	27–30 km (30–37%)	175 km	Paleocene to Eocene
Kraemer (2003)	19 km (11%)	13 km (10%)	170 km	Paleogene
Torres Carbonell and Dimieri (2013)	–	46 km (48%)	40 km	Paleocene to Miocene in six stages
Torres Carbonell et al. (2017)	62 km (40%)	59 km (49%)	120 km	Paleocene to Miocene
Lozano et al. (2020)	–	16.6 km (38.4%)	83 km	Paleocene to Miocene

building of the MMFTB in Tierra del Fuego onshore and offshore. Herein, we presented depth maps of the basement top with the basement-involved faults and top of predeformational Oligocene levels. Several seismic lines interpreted both in onshore and offshore regions were also presented, together with an estimation of the shortening associated with the formation of the Géminis anticline in offshore.

This work supports that the formation of the MMFTB was substantially conditioned by the buttressing effect exerted by the Río Chico Arch, and a series of basement steps. The buttressing effect is centred at the vertex of the Río Chico Arch, located at 67° W, as indicated by the change of direction of folds, converging around this feature. The apex of the Río Chico Arch concentrates the greater shortening of the MMFTB, with a decreased amount of shortening both towards east and west.

The coincidence in strike and location of folds with basement-involved faults in the most external part of the FTB is due to a connection between them. These basement steps are Mesozoic structures, bounded by extensional faults. The largest of these features is located in the foredeep, as part of a negative flower structure, formed during the Paleocene-Eocene transtensional processes. This structure appears toward the east of the studied area and is more developed eastwards towards Malvinas basin. The inversion of the flower structure during the late Oligocene/lower Miocene compression resulting in Cicłón anticline formation seems to be the most likely scenario.

The Géminis anticline is a fault propagation fold developed over a basement-involved fault in the most external part of the MMFTB. This fault acted as a stress riser, controlling both the location of the Géminis anticline, and the piggyback basin developed over its backlimb.

The history of the area initiates with the faulting of the Paleozoic basement during the Mesozoic rifting processes in Magallanes and Malvinas basins. A relatively unfaulted basement high, the Río Chico Arch, remained between the basins. This mechanical rifting led to the generation of half grabens, which were filled during the Mesozoic,

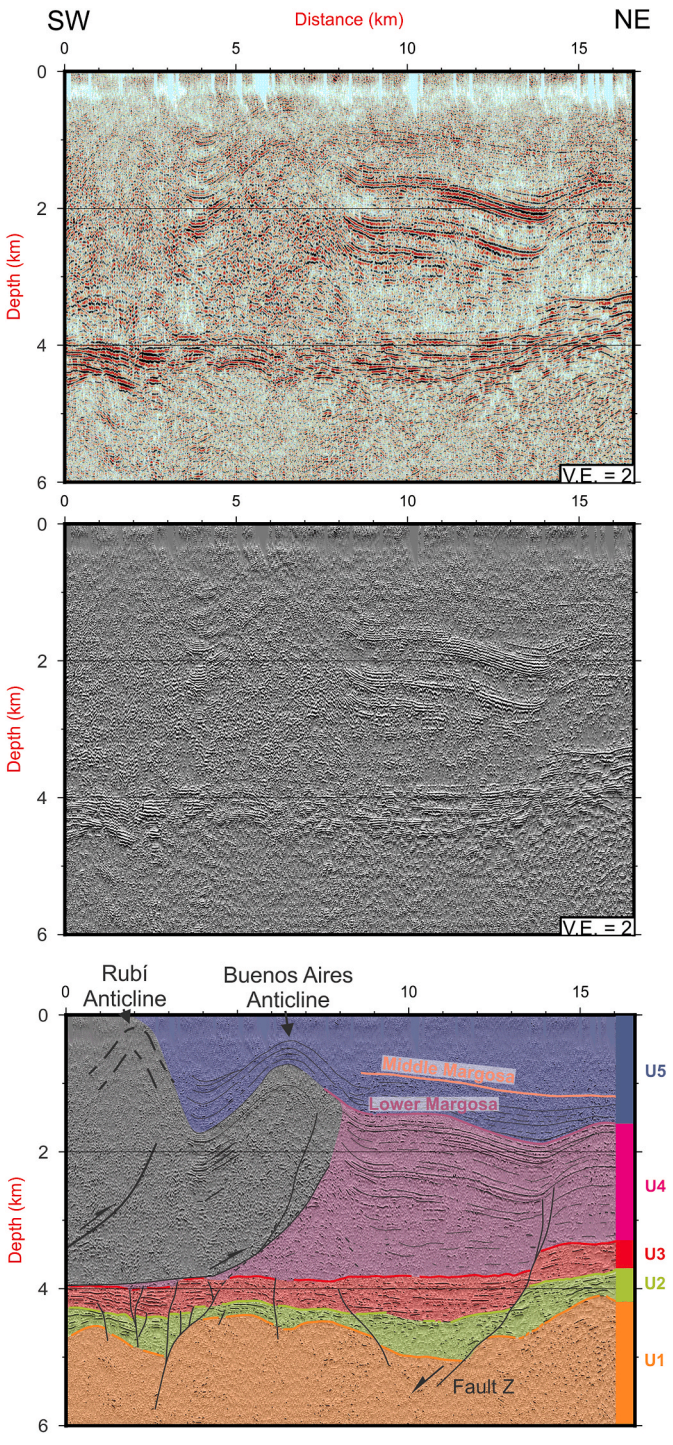

Fig. 12. Onshore multichannel Seismic line (upper) processed with TecVA (middle, Bulhões and de Amorim, 2005) and interpretation (below). Units interpretation, and Buenos Aires anticline with associated basement-involved faults after Torres Carbonell et al. (2017). V.E: Vertical Exaggeration. See location in Fig. 4.

followed by a sag phase. Since the Upper Cretaceous, when a compression regime was established, basins inversion and rising of the Fuegian Cordillera took place. Eastwards of the Río Chico Arch, towards Malvinas Basin, a transtensional tectonic phase was active in Paleocene-Eocene times, configuring a series of flower structures. Since the middle Eocene, the entire region was affected by a compressional tectonic phase. This compression generated the formation of the Magallanes-Malvinas Fold and Thrust Belt and was active until the late Oligocene/early Miocene. The anticlines Géminis and Ciclón were formed during this phase, with a location conditioned by the presence of basement-involved faults. After the deactivation of the FTB, the region is under a counterclockwise strike-slip regime.

Declaration of competing interest

The authors declare that they have no known competing financial interests or personal relationships that could have appeared to influence the work reported in this paper.

CRediT authorship contribution statement

J.P. Ormazabal: Conceptualization, Methodology, Software, Writing - original draft. **J.I. Isola:** Visualization, Writing - review & editing. **F.I. Palma:** Writing - review & editing. **J.G. Lozano:** Methodology, Validation. **F.D. Esteban:** Methodology, Software. **M.M. Menichetti:** Writing - review & editing. **E. Lodolo:** Writing - review & editing. **A.A. Tassone:** Writing - review & editing, Supervision, Funding acquisition, Project administration.

Acknowledgments

This work has been made within the framework of a collaboration between YPF technology S.A. (Y-TEC) and the Consejo Nacional de Investigaciones Científicas y Técnicas (CONICET). The authors express their thanks to YPF S.A. for their constant support. This contribution is framed within the Pampa Azul project, which is funded by the Ministry of Science Technology and Productive Innovation of Argentina (MINCyT). The Secretaría de Energía Argentina is thanked for providing the multichannel seismic and well data interpreted in this work. Special thanks to Sonia Sanchez for her helping with improving English writing of this work. Eloy Mendoza is thanked for his helping with seismic processing. Finally, we are grateful for the constructive reviews made by two anonymous reviewers, which greatly helped to improve the original manuscript, and the evaluation of this work and dedication by the Editors Dr. Folguera and Dr. Martínez.

References

Alvarez-Marrón, J., McClay, K.R., Harambour, S., Rojas, L., Skarmeta, J., 1993. Geometry and evolution of the frontal part of the Magallanes foreland thrust and fold belt (Vicuna area), Tierra del Fuego, southern Chile. AAPG (Am. Assoc. Pet. Geol.) Bull. 77 (11), 1904–1921.

Baristeas, N., Anka, Z., Di Primio, R., Rodriguez, J.F., Marchal, D., Dominguez, F., 2013. New insights into the tectono-stratigraphic evolution of the Malvinas Basin, offshore of the southernmost Argentinean continental margin. Tectonophysics 604, 280–295.

Biddle, K.T., Uliana, M.A., Mitchum, R.M., Fitzgerald, M.G., Wright, R.C., 1986. The Stratigraphic and Structural Evolution of the Central and Eastern Magallanes Basin. southern South America, Foreland basins, pp. 41–61.

Bulhões, É.M., de Amorim, W.N., 2005. Princípio da Sismo Camada Elementar e sua aplicação à Técnica Volume de Amplitudes (tecVA). In: 9th International Congress of the Brazilian Geophysical Society and EXPOGEF, Salvador, Bahia, Brazil, 11-14 September 2005, vol. 2005. Society of Exploration Geophysicists and Brazilian Geophysical Society, pp. 1382–1387.

Cagnolatti, M., Covellone, G., Erlicher, J., Fantín, F., 1987. Fallamiento y plegamiento de cobertura al suroeste del Río Grande, Cuenca Austral, Tierra del Fuego, Argentina. In: X Congreso Geológico Argentino, pp. 149–152.

Diraison, M., Cobbold, P.R., Gapais, D., Rossello, E.A., Gutiérrez Pleimling, A., 1997. Neogene tectonics within the magellan basin (Patagonia). 6 simposio bolivariano (petroleum exploration in the subandean basins). Cartagena de Indias, Colombia Memorias 1, 1–14.

Diraison, M., Cobbold, P.R., Gapais, D., Rossello, E.A., Le Corre, C., 2000. Cenozoic crustal thickening, wrenching and rifting in the foothills of the southernmost Andes. Tectonophysics 316 (1-2), 91–119.

Esteban, F.D., 2014. Estudio geofísico-geológico del subsuelo del segmento noroccidental de la Dorsal Norte del Scotia. Ph. D. thesis. Universidad de Buenos Aires, Argentina.

Esteban, F.D., Tassone, A., Isola, J., Lodolo, E., Menichetti, M., 2018. Geometry and structure of the pull-apart basins developed along the western South American-Scotia plate boundary (SW Atlantic Ocean). J. S. Am. Earth Sci. 83, 96–116.

Flores, M.A., Malumián, N., Masiuk, V., Riggi, J.C., 1973. Estratigrafía cretácica del subsuelo de Tierra del Fuego. Rev. Asoc. Geol. Argent. 28, 407–437.

Galeazzi, J.S., 1998. Structural and stratigraphic evolution of the western Malvinas basin, Argentina. AAPG (Am. Assoc. Pet. Geol.) Bull. 82 (4), 596–636.

Géminis x-1, 2004. Geological End of Well Report. Total, p. 72 (Unpublished).
Ghiglione, M.C., 2002. Diques clásticos asociados a deformación transcurrente en depósitos sinorogénicos del Mioceno inferior de la Cuenca Austral. Rev. Asoc. Geol. Argent. 57 (2), 103–118.
Ghiglione, M.C., Ramos, V.A., 2005. Progression of deformation and sedimentation in the southernmost Andes. Tectonophysics 405 (1-4), 25–46.
Ghiglione, M.C., Yagupsky, D., Ghidella, M., Ramos, V.A., 2008. Continental stretching preceding the opening of the Drake Passage: evidence from Tierra del Fuego. Geology 36 (8), 643–646.
Ghiglione, M.C., Quinteros, J., Yagupsky, D., Bonillo-Martínez, P., Hlebszevtich, J., Ramos, V.A., Vergani, G., Figueroa, D., Quesada, S., Zapata, T., 2010. Structure and tectonic history of the foreland basins of southernmost South America. J. S. Am. Earth Sci. 29 (2), 262–277.
Ghiglione, M.C., Navarrete-Rodríguez, A.T., González-Guillot, M., Bujalesky, G., 2013. The opening of the Magellan Strait and its geodynamic implications. Terra. Nova 25 (1), 13–20.
Klepeis, K.A., Austin, J.A., 1997. Contrasting styles of superposed deformation in the southernmost Andes. Tectonics 16 (5), 755–776.
Kley, J., Monaldi, C.R., Salfity, J.A., 1999. Along-strike segmentation of the Andean foreland: causes and consequences. Tectonophysics 301 (1-2), 75–94.
Kraemer, P.E., 2003. Orogenic shortening and the origin of the Patagonian orocline (56 S. Lat). J. S. Am. Earth Sci. 15 (7), 731–748.
Lodolo, E., Menichetti, M., Tassone, A., Geletti, R., Sterzai, P., Lippai, H., Hormaechea, J. L., 2002. Researchers target a continental transform fault in Tierra del Fuego. Eos, Transactions American Geophysical Union 83 (1), 1–6.
Lozano, J.G., Bran, D.M., Peroni, J.I., Lodolo, E., Menichetti, M., Cerredo, M.E., Tassone, A., 2020. The central Fuegian fold and thrust belt in Tierra del Fuego: strike-slip tectonics superimposed onto compressional deformation. Geol. J. 1–19.
Maestro, A., Ruano, P., Torres Carbonell, P., Bohoyo, F., Galindo-Zaldívar, J., Pedrera, A., Ruiz-Constán, A., González-Castillo, L., Ibarra, P., López-Martínez, J., 2019. Stress field evolution of the southernmost Andean Cordillera from paleostress analysis (Argentine Tierra del Fuego). Tectonics 38 (1), 7–25.
Malumián, N., Olivero, E.B., 2006. El Grupo Cabo Domingo, Tierra del Fuego, Argentina: bioestratigrafíaa, paleoambientes y acontecimientos del Eoceno- Mioceno marino. Rev. Asoc. Geol. Argent. 61, 139–160.
Masiuk, V., Riggi, J.C., Bianchi, J.L., 1990. Análisis geológico del Terciario del subsuelo de Tierra del Fuego. Bol. Inf. Pet. (1924) 21, 70–89.
Menichetti, M., Lodolo, E., Tassone, A., 2008. Structural geology of the Fuegian Andes and Magallanes fold and thrust belt - Tierra del Fuego Island. Geol. Acta 6 (1), 19–42.
Olivero, E.B., Malumián, N., 1999. Eocene stratigraphy of southeastern Tierra del Fuego island, Argentina. AAPG Bull. 83 (2), 295–313.
Olivero, E.B., Malumián, N., 2008. Mesozoic-cenozoic stratigraphy of the fuegian Andes, Argentina. Geol. Acta 6, 5–18.
Olivero, E.B., Malumián, N., Palamarczuk, S., Scasso, R.A., 2002. El Cretácico superior-Paleógeno del área del Río Bueno, costa atlántica de la Isla Grande de Tierra del Fuego. Rev. Asoc. Geol. Argent. 57, 199–218.
Ormazabal, J.P., Tassone, A., Esteban, F., Isola, J., Cayo, L.E., Lozano, J., Menichetti, M., Lodolo, E., 2019. Structure of the wedge-top and foredeep of the Magallanes-Malvinas basins between 62° W and 67° W (SW atlantic ocean). J. S. Am. Earth Sci. 93, 364-38.
Rojas, L., Mpodozis, C., 2006. Geología estructural de la Faja Plegada y Corrida del sector chileno de Tierra del Fuego, Andes patagónicos australes. In: Congreso Geológico Chileno No. 11: Actas, vol. 1.
Robbiano, J.A., Arbe, H., Gangui, A., 1996. Cuenca austral marina. In: Ramos, V.A., Turic, M.A. (Eds.), Geología y Recursos Naturales de la Plataforma Continental Argentina. 13° Congreso Geológico Argentino, y 3° Congreso de Exploración de Hidrocarburos. Relatorio, pp. 323–342 (Buenos Aires).
Sachse, V.F., Strozyk, F., Anka, Z., Rodriguez, J.F., Di Primio, R., 2016. The tectono-stratigraphic evolution of the Austral Basin and adjacent areas against the background of Andean tectonics, southern Argentina, South America. Basin Res. 28 (4), 462–482.
Tassone, A., Lodolo, E., Menichetti, M., Yagupsky, D.L., Caffau, M., Vilas, J.F.A., 2008. Seismostratigraphic and structural setting of the Malvinas Basin and its southern margin (Tierra del Fuego Atlantic offshore). Geol. Acta 6 (1), 55–67.
Torres Carbonell, P.J., Dimieri, L.V., 2013. Cenozoic contractional tectonics in the Fuegian Andes, southernmost South America: a model for the transference of orogenic shortening to the foreland. Geol. Acta 11 (3), 331–357.
Torres Carbonell, P.J., Olivero, E.B., 2019. Tectonic control on the evolution of depositional systems in a fossil, marine foreland basin: example from the SE Austral Basin, Tierra del Fuego, Argentina. Mar. Petrol. Geol. 104, 40–60.
Torres Carbonell, P.J., Olivero, E.B., Dimieri, L.V., 2008. Structure and evolution of the Fuegian Andes foreland thrust-fold belt, Tierra del Fuego, Argentina: paleogeographic implications. J. S. Am. Earth Sci. 25 (4), 417–439.
Torres Carbonell, P.J., Dimieri, L.V., Olivero, E.B., 2011. Progressive deformation of a coulomb thrust wedge: the eastern fuegian Andes thrust-fold belt. Geological Society, London, Special Publications 349 (1), 123–147.
Torres Carbonell, P.J., Dimieri, L.V., Martinioni, D.R., 2013. Early foreland deformation of the Fuegian Andes (Argentina): constraints from the strain analysis of Upper Cretaceous-Danian sedimentary rocks. J. Struct. Geol. 48, 14–32.
Torres Carbonell, P.J., Dimieri, L.V., Olivero, E.B., Bohoyo, F., Galindo-Zaldívar, J., 2014. Structure and tectonic evolution of the fuegian Andes (southernmost South America) in the framework of the Scotia arc development. Global Planet. Change 123, 174–188.
Torres Carbonell, P.J., Rodríguez Arias, L., Atencio, M.R., 2017. Geometry and kinematics of the Fuegian thrust-fold belt, southernmost Andes. Tectonics 36 (1), 33–50.
Wessel, P., Smith, W.H.F., Scharroo, R., Luis, J., Wobbe, F., 2013. Generic mapping Tools: improved version released. Eos, Trans. Am. Geophys. Union 94 (45), 409–410.
Yrigoyen, M.R., 1989. Cuenca de Malvinas. Cuencas Sedimentarias Argentinas. Universidad Nacional de Tucumán, Serie Correlación Geológica 6, 481–491.